



Interactions of dipalmitoylphosphatidylcholine with ceramide-based mixtures

G.S. Gooris^a, M. Kamran^a, A. Kros^b, D.J. Moore^c, J.A. Bouwstra^{a,*}

^a Leiden Academic Centre for Drug Research, Leiden University, Gorlaeus laboratories, 2333 CC Leiden, The Netherlands

^b Leiden Institute of Chemistry, Leiden University, Gorlaeus laboratories, 2333 CC Leiden, The Netherlands

^c GSK Consumer Healthcare, 184 Liberty Corner Road, Warren, NJ, United States of America

ARTICLE INFO

Keywords:

Lipid organization
Stratum corneum
Lipid composition
Phospholipids
Ceramides

ABSTRACT

The outermost layer of the skin, the stratum corneum (SC), acts as the natural physical barrier. The SC consists of corneocytes embedded in a crystalline lipid matrix consisting of ceramides, free fatty acids and cholesterol.

Although phospholipids are frequently present in topical formulations, no detailed information is reported on the interactions between phospholipids and SC lipids. The aim of this study was to examine the interactions between a model phospholipid, dipalmitoylphosphatidylcholine (DPPC) and synthetic ceramide-based mixtures (referred to as SC lipids).

(Perdeuterated) DPPC was mixed with SC lipids and the lipid organization and mixing properties were examined. The studies revealed that DPPC participates in the same lattice as SC lipids thereby enhancing a hexagonal packing. Even at a high DPPC level, no phase separated pure DPPC was observed.

When a DPPC containing formulation is applied to the skin surface it must partition into the SC lipid matrix prior to any mixing with the SC lipids. To mimic this, DPPC was applied on top of a SC lipid membrane. DPPC applied in a liquid crystalline state was able to mix with the SC lipids and participated in the same lattice as the SC lipids. However, when DPPC was applied in a rippled gel-state very limited partitioning of DPPC into the SC lipid matrix occurred. Thus, when applied to the skin, liquid crystalline DPPC will have very different interactions with SC lipids than DPPC in a (rippled-)gel phase.

1. Introduction

Several therapeutic and cosmetic formulations for topical skin health applications on the market contain phospholipids, most commonly phosphatidylcholine (lecithin). In general liquid crystalline phosphatidylcholine is utilized to form liposomes although phospholipids are also used as natural emulsifiers [1]. Very little information has been reported describing the interaction between phospholipids (particularly conformationally ordered phosphatidylcholine) and skin barrier lipids. In this work the interaction between dipalmitoyl phosphatidyl choline (DPPC) and two skin barrier lipid models was examined using Fourier transform infrared spectroscopy (FTIR) and X-ray diffraction. DPPC was selected as it is one of the most frequently used phospholipids and exists in an ordered gel phase at skin physiological temperatures (~32 °C).

The skin is composed of several morphologically distinct layers. The upper layer of the skin is the stratum corneum (SC). Human SC is a 10–15 μm thick layer consisting of corneocytes in a lipid matrix, which is responsible for the primary skin barrier function. The corneocytes are flat hexagonal-shaped dead cells, covalently linked together by corneodesmosomes, and filled with keratin filaments, bound water and hygroscopic molecules known as natural moisturising factor [2]. The free volume between corneocytes is filled with three major classes of lipids; free fatty acids (FFAs), ceramides (CERs) and cholesterol (CHOL) [3]. As the extra-cellular lipid domains form a continuous structure in the SC, molecules diffusing across the SC always have to pass through the lipid regions. For this reason, the SC lipids play an important role in skin barrier function and the arrangement of the lipids in lamellar domains is a key process in the formation of the skin barrier. X-ray diffraction studies of human SC have shown that the lipids are arranged in

Abbreviations: SC, stratum corneum; CER, ceramide; CHOL, cholesterol; FFA, free fatty acid; FTIR, Fourier transformed infrared spectroscopy; SAXD, small angle X-ray diffraction; FA24, lignoceric acid; DPPC, dipalmytoyl phosphatidyl choline; EOS, ester linked omega-hydroxy acyl chain linked to a sphingosine chain; NS, a non-hydroxy acyl chain linked to a sphingosine base; SPP, short periodicity phase; LPP, long periodicity phase

* Corresponding author at: Division of Drug Delivery Technology, Cluster BioTherapeutics, Leiden Academic Centre for Drug Research, Leiden University, Gorlaeus Laboratories, Einsteinweg 55, 2333 CC Leiden, The Netherlands.

E-mail address: bouwstra@chem.leidenuniv.nl (J.A. Bouwstra).

<https://doi.org/10.1016/j.bbamem.2018.02.024>

Received 12 October 2017; Received in revised form 22 February 2018; Accepted 26 February 2018

Available online 28 February 2018

0005-2736/ © 2018 The Authors. Published by Elsevier B.V. This is an open access article under the CC BY license (<http://creativecommons.org/licenses/by/4.0/>).

two crystalline lamellar phases with repeat distances of 6 (short periodicity phase, SPP) and 13 nm (long periodicity phase, LPP), respectively [4]. The 2-dimensional crystalline packing of the lipid methylene groups is mainly orthorhombic, although a fraction of lipids also exhibits a hexagonal packing. The SC lipid domains are also very important when studying and interpreting the interaction of exogenous compounds with the SC. Several studies have reported on a range of interactions between chemical penetration enhancers and a range of emollient molecules with SC lipids [5–7].

While the SC is comprised of only three major lipid classes, the composition is very complex at the sub-class and species level. To date approximately 17 CER subclasses and 3 FFA subclasses have been identified in human SC [8–11]. Furthermore, each of these subclasses has a wide variation in chain length distribution. Consequently there are more than 1000 chemically distinct lipids in the SC. Recently we observed that a less complex well-defined lipid composition consisting of a limited number of CER subclasses, CHOL and the most abundant FFA assembles in both the LPP and the SPP [12] while adopting a predominantly orthorhombic packing at room temperature [12,13]. This has also been encountered in many other mixtures prepared with CERs, in which the mixing properties were strongly affected by lipid chain length distribution [14–16].

In this work, three or four component mixtures were selected that are able to form either the SPP or the LPP, respectively. For these mixtures we used synthetic ceramides. To determine the interactions between DPPC and SC lipids, the lipids were mixed with gradually increasing level of (perdeuterated) DPPC. We observed that high levels of DPPC are able to mix with the SC lipids and appear to participate in the same lattice as the SC lipids. To examine the partitioning of DPPC in a preformed SC lipid layer, a DPPC layer was placed on top of a SC lipid membrane and the partitioning and mixing of DPPC with the SC lipids was examined as a function of the DPPC phase behaviour (rippled gel phase or liquid crystalline ($L\alpha$) phase) [17]. These studies show that DPPC in liquid crystalline phase can partition into the SC lipid membrane and “mix” with the SC lipids.

2. Experimental section

2.1. Materials

Two synthetic CERs were used in our studies: 1) *N*-(omega-linoleoyl) sphingosine (abbreviation CER EOS) with an acyl chain of 30 carbon atoms and a sphingosine of 18 carbons, 2) a non-hydroxy acyl chain sphingosine (abbreviation CER NS). The acyl chain is 24 carbons and the sphingosine 18 carbons. For the molecular architecture of the CERs, see Supplement S1. The CERs were kindly provided by Evonik (Essen, Germany). Lignoceric acid (FA24) and CHOL were obtained from Sigma-Aldrich Chemie GmbH (Schnellendorf, Germany). DPPC and perdeuterated DPPC was purchased from Avanti Polar Lipids (Alabaster, AL). Nuclepore polycarbonate filter disks with pore size of 50 nm were obtained from Whatman (Kent, UK). All solvents were of analytical grade and supplied by Labscan (Dublin, Ireland). The water used was of Millipore quality produced by Milli-Q water filtration system.

2.2. Preparation of the model lipid mixtures

The SC lipid mixtures were prepared using equimolar ratios of CER:CHOL:FA24. The CER consisted either of two CER subclasses, CER EOS and CER NS in a molar ratio of 40:60 (referred to as CER EOS/NS) or a single CER subclass, CER NS. Mixtures were prepared with a gradual increased level of (perdeuterated) DPPC varying in a molar ratio between CER:CHOL:FA24:DPPC = 1:1:1:0 to 1:1:1:4.

In preparing the model lipid mixtures, the appropriate amount of individual lipids was dissolved in chloroform:methanol (2:1) at a final concentration of 5 mg/ml and sprayed under a stream of nitrogen on a

AgBr window using a Linomat IV (Camag, Muttenz, Switzerland). The Linomat device makes use of a Hamilton syringe (100 μ l) and mechanics to spray a programmable volume of sample solution on either nucleopore filter disks (X-ray diffraction) or a AgBr window (Fourier transform infrared spectroscopy, FTIR). With the y-axis arm, the linomat is capable of spraying lipids in a rectangular shape. The spraying flow rate is 5.0 μ l/min under a stream of nitrogen gas at a movement speed of 1 cm/s. After spraying, the lipid samples were equilibrated for 10 min at 85 °C. Then the mixture was cooled in approximately 30 min. Subsequently, the lipid layer was covered with 25 μ l of a 50 mM acetate buffer (prepared with D₂O for FTIR studies) at pH 5. After buffer application, the sample was kept at 37 °C overnight to obtain a full hydration [18].

2.3. Fourier transform infrared spectral measurements

All spectra were measured on a Varian 670-IR FTIR or a Biorad FTS4000 FTIR spectrometer (Cambridge Massachusetts) equipped with a broad-band mercury cadmium telluride detector. The detector was cooled by liquid nitrogen. The sample cell was closed by two AgBr windows. The sample was under continuous dry air purge starting 1 h before the data acquisition. The spectra were measured in transmission mode. Each measurement consisted of a co-addition of 256 scans in a time period of 4 min. The resolution was 1 cm^{-1} . The thermotropic response was examined by increasing the sample temperature at a heating rate of 0.25 °C/min resulting in a 1 °C temperature rise per recorded spectrum until a temperature of 90 °C was reached. The software used was Resolutions Pro 4.1.0. from Varian.

2.4. Small-angle x-ray diffraction measurements

Small-angle x-ray diffraction (SAXD) was used to obtain information about the lamellar organization (i.e., the repeat distance of a lamellar phase). The scattering intensity I (in arbitrary units) was measured as function of the scattering vector q (in reciprocal nm). The latter is defined as $q = (4\pi\sin\theta) / \lambda$, in which θ and λ are the scattering angle and wavelength, respectively. From the positions of a series of equidistant peaks (q_n), the periodicity (d) of a lamellar phase was calculated using the equation $d = 2n\pi / q_n$, with n being the order number of the diffraction peak. One-dimensional intensity profiles were obtained by transformation of the 2D SAXD detector pattern from Cartesian (x, y) to polar (ρ, θ) coordinates and subsequently integrating over θ . All measurements were performed at the European Synchrotron Radiation Facility (ESRF, Grenoble) using station BM26B [19]. The wavelength of the X-ray and the sample-to-detector distance were 0.1033 nm and 2.1 m, respectively. The diffraction data were collected on a PILATUS 1M detector (1043 \times 981 pixels) and 172 μ m spatial resolution. The calibration of this detector was performed using silver behenate and aluminium oxide. The lipid membrane was mounted parallel to the primary beam in a sample holder with mica windows. All the diffraction data were collected for about 5 min at 25 °C.

2.5. Dynamic measurements

In addition to the mixing of DPPC and SC lipids in the organic solvent and subsequently spraying this mixture onto the support, the ability of DPPC to penetrate into a SC lipid membrane was also assessed. To examine this, DPPC was sprayed on one AgBr window using the same method as described above. The CER EOS/NS:CHOL:FA24 equimolar mixture was sprayed on another AgBr window. The skin lipid mixture was equilibrated at elevated temperatures (85 °C) and cooled to room temperature. Subsequently both, the skin lipid mixture and the DPPC, were hydrated overnight at 37 °C using an acetate buffer (pH 5). The excess water was removed and the two windows were sealed in the FTIR sample cell. The temperature of the cell was increased to either 32 or 37 °C, after having reached this temperature, the membrane was kept

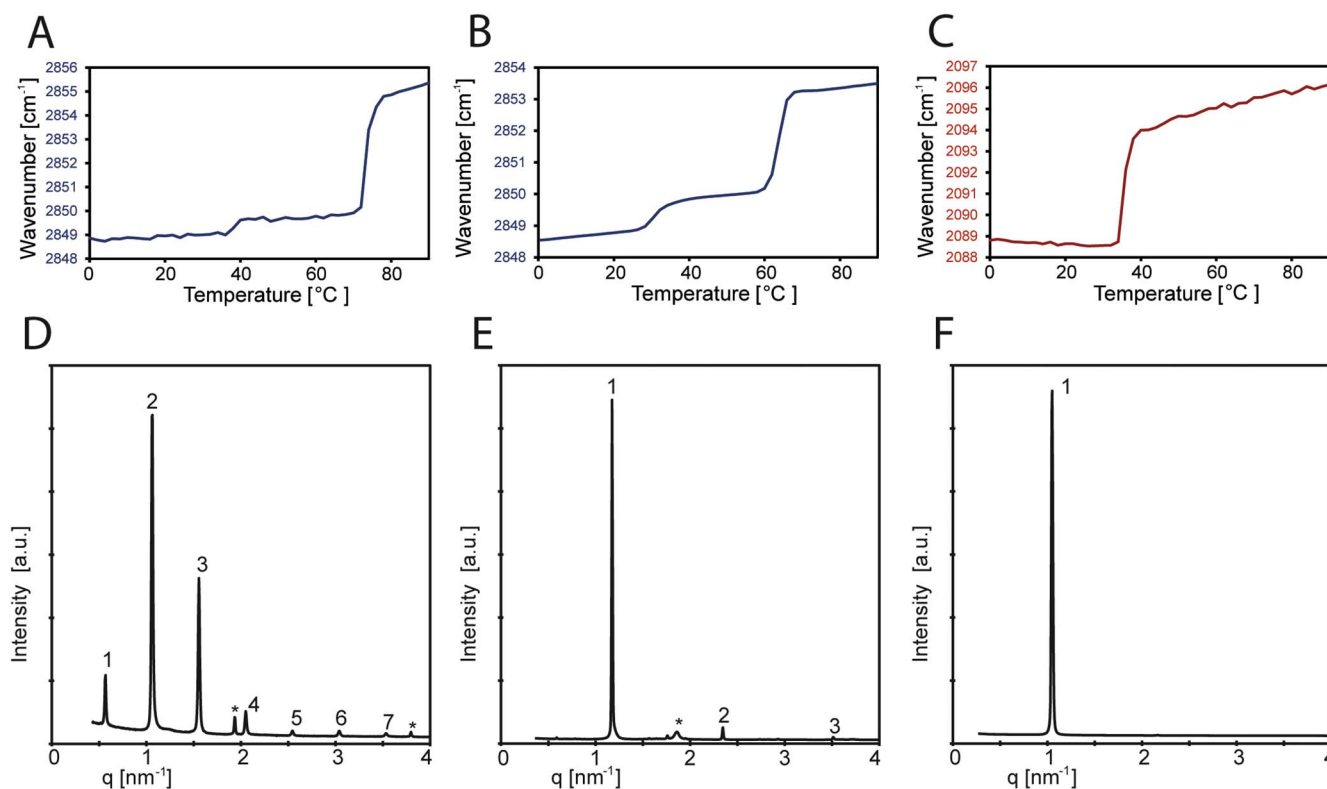


Fig. 1. The CH₂ stretching thermotropic response of the A) equimolar CER EOS/NS:CHOL:FA24 mixture, B) equimolar CER NS:CHOL:FA24 mixture and C) Perdeuterated DPPC. Both skin lipid mixtures exhibit two shifts in CH₂ stretching frequencies indicating two transitions at around 35 and 60 °C: the orthorhombic to hexagonal and hexagonal to liquid phase transition. The CD₂ stretching thermotropic response of DPPC indicates only one shift at around 32 °C. D) The X-ray diffraction curve of the equimolar CER EOS/NS:CHOL:FA24 mixture, the reflections attributed to the LPP with a repeat distance of 12.3 nm are located at q value of 0.50, 1.00, 1.50 and 2.00 nm⁻¹ and E) The X-ray diffraction curve of the equimolar CER NS:CHOL:FA24 mixture, the reflections attributed to the SPP with a repeat distance of 5.3 nm are located at q-values of 1.17 and 2.34 nm⁻¹. The X-ray diffraction curve of hydrated DPPC is provided in panel F. A strong reflection is observed at 1.1 nm⁻¹, indicating a repeat distance of 5.8 nm.

at a fixed temperature for 12 or 24 h. Subsequently, FTIR spectra were recorded between 0 and 90 °C as described above.

3. Results

3.1. Mixing of DPPC with SC lipids: interaction of DPPC with lipids that assemble in the LPP

3.1.1. Skin lipid mixtures and pure DPPC

FTIR studies were performed using either CER EOS/NS:CHOL:FA24, CER NS:CHOL:FA24 mixture or pure DPPC. First CH₂ symmetric stretching bands were monitored as a function of temperature. These bands are a signature for the conformational ordering of the lipids. The thermotropic response of the CH₂ stretching vibrations between 0 and 90 °C of both SC lipid compositions and perdeuterated DPPC are provided in Fig. 1. In both mixtures at 10 °C the CH₂ stretching vibration wavenumber is around 2848.9 cm⁻¹, indicating an all-trans conformation of the chains [20,21]. The orthorhombic to hexagonal phase transition is indicated by a small shift (less than 1 cm⁻¹) in wavenumber between 30 and 40 °C. The hexagonal-liquid phase transition is detected by a large shift (larger than 3 cm⁻¹) in the stretching frequencies at much higher temperatures. The midpoint temperature of the orthorhombic to hexagonal transition are 35 °C and 30 °C for the CER EOS/NS:CHOL:FA24 and CER NS:CHOL:FA24 mixtures, respectively. For the hexagonal to liquid phase the mid-transition temperature is 73.3 °C and 64 °C for the CER EOS/NS:CHOL:FA24 and CER NS:CHOL:FA24 mixtures, respectively. The thermotropic response of the CD₂ stretching frequencies of perdeuterated DPPC is also provided in Fig. 1: Only a strong shift occurs with a midpoint transition at around 36 °C indicating a rippled-gel to liquid phase transition [17]. The long range ordering of the SC lipids are also plotted in Fig. 1. The X-ray

diffraction curve of CER EOS/NS:CHOL:FA24 shows a large series of reflections (1st, 2nd, 3rd, 4th, 5th, 6th and 7th order) attributed to the LPP. Two additional peaks are attributed to phase separated CHOL. The repeat distance of the LPP calculated from the positions of the reflections is 12.3 nm. The X-ray diffraction curve of CER NS:CHOL:FA24 reveals three diffraction peaks attributed to the SPP with a repeat distance of 5.3 nm, The repeat distance was calculated from the positions of the diffraction peaks and was 5.8 nm.

3.1.2. Mixing of (perdeuterated) DPPC with SC lipids: interaction with SC lipids that assemble in the LPP

Lipid mixtures with a gradual increase in DPPC level were examined. First we focused on the transition temperature of the hexagonal-liquid phase transition determined by the CH₂ and CD₂ symmetric stretching vibrations monitored between 0 and 90 °C. Perdeuterated DPPC was mixed with the SC lipids at ratios varying between CER EOS/NS:CHOL:FA24:DPPC 1:1:1:0.2 and 1:1:1:4 as depicted in Fig. 2. The wavenumbers of the CH₂ symmetric stretching vibration were increased at 10 °C compared to the 1:1:1:0, except for the 1:1:1:0.6 M ratio, see Table 1, while the midrange temperature of the hexagonal to liquid phase-transition is lower than in the 1:1:1:0 M ratio. Furthermore, as shown by the CH₂ and CD₂ thermotropic response curves, the hexagonal to liquid phase transition of DPPC and SC lipids occurs in the same temperature regions, while no shift in CD₂ wavenumber is observed at 35 °C, the rippled-gel to liquid phase transition of pure perdeuterated DPPC. This is a first indication that DPPC is mixing with the SC lipids.

For more detailed information on the lateral packing and mixing properties we primarily focused on the CH₂ and CD₂ scissoring vibrations. If the CH₂ scissoring band is a singlet, the lipids form either a liquid or a hexagonal lateral packing and the peak position is at

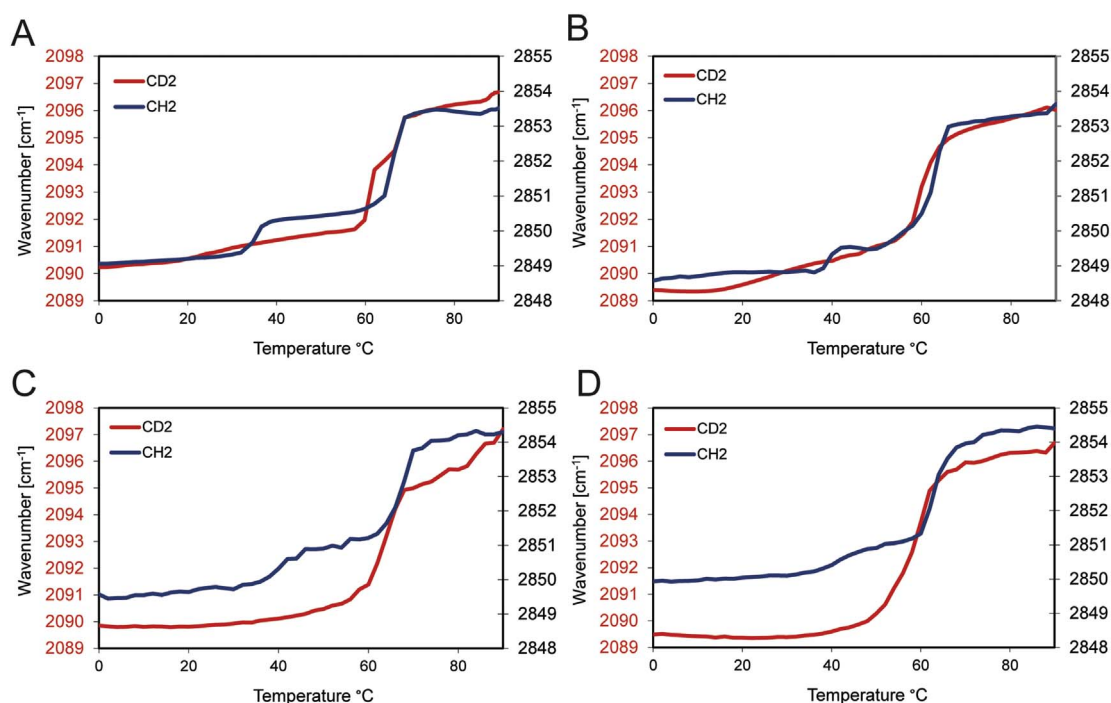


Fig. 2. The CH₂ and CD₂ symmetric stretching vibrations of CER EOS/NS:CHOL:FA24 with increasing level of perdeuterated DPPC. A) CER EOS/NS:CHOL:FA24:DPPC = 1:1:1:0.2, (B) CER EOS/NS:CHOL:FA24:DPPC = 1:1:1:0.6, (C) CER EOS/NS:CHOL:FA24:DPPC = 1:1:1:1 and (D) CER EOS/NS:CHOL:FA24:DPPC = 1:1:1:4.

Table 1

The CH₂ symmetric stretching vibrations at 10 °C together with the midrange transition temperatures (T_m) of the hexagonal to liquid transition for the CER EOS/NS:CHOL:FA24:DPPC mixtures.

CER EOS/NS:CHOL:FA24:DPPC	DPPC mole fraction	CH ₂ stretching (cm ⁻¹)	T _m (°C)
1:1:1:0.2	0.063	2849.1	66.4
1:1:1:0.6	0.167	2848.7	62.9
1:1:1:1	0.250	2849.6	67.1
1:1:1:4	0.571	2850.1	63.2

1467 cm⁻¹. When lipids form an orthorhombic packing, chains in scissoring modes interact via a short-range coupling resulting in a broadening or splitting of the contours [20]. When maximal splitting occurs, indicating domains containing at least 100 lipids adopting an orthorhombic packing, the peak positions are at 1463 cm⁻¹ and 1474 cm⁻¹. When deuterated chains are intercalated in the orthorhombic lattice, no coupling occurs between the deuterated and protiated chains. This enhances the formation of a single scissoring contour in the IR spectrum at 1467 cm⁻¹. Therefore, these modes can be used to determine whether deuterated chains participate in the same lattice as the protiated ones that form an orthorhombic x-y plane lattice.

In Fig. 3 the scissoring frequencies of the CH₂ scissoring modes are shown for the equimolar mixture CER EOS/NS:CHOL:FA24. A clear splitting of the peaks was observed at low temperatures demonstrating that the orthorhombic packing is prominently present in this mixture. A transition occurred between 32 °C and 42 °C: in this temperature region the two scissoring frequencies turned into a single scissoring mode at 1467 cm⁻¹, indicative for an orthorhombic-hexagonal phase transition. After addition of perdeuterated DPPC resulting in a CER EOS/NS:CHOL:FA24:DPPC composition of 1:1:1:0.2M ratio, there was hardly no change in the CH₂ scissoring contours in the spectrum. Increasing the level of perdeuterated DPPC to a ratio of 1:1:1:0.6 resulted in the appearance of a central weak peak at 1467 cm⁻¹. Simultaneously the intensity was reduced of the two scissoring frequencies at 1463 and 1473 cm⁻¹ at low temperature compared to the scissoring contours in

the spectrum of the 1:1:1:0.2 mixture. This indicates that DPPC is at least partly participating in the same lattice as the SC lipids. The slight asymmetry in the intensity of the peaks may indicate that a part of the lipids are in a distorted orthorhombic packing [22]. A further increase in the level of perdeuterated DPPC increased the intensity of this central contour compared to that in the spectrum of the 1:1:1:0.6 mixture. The spectrum of CER EOS/NS:CHOL:FA24:DPPC at a ratio of 1:1:1:4 depicted a strong contour at 1467 cm⁻¹, while the areas of the two bands attributed to the orthorhombic lateral packing were further reduced. Interestingly, the temperature region of orthorhombic to hexagonal phase transition was very similar in all mixtures.

These studies demonstrate that DPPC is at least partly participating in the same lattice as the SC lipids. However, whether this lattice is only orthorhombic or that lipids also participate in a hexagonal lateral packing cannot be deduced from these spectra. In order to determine this we also examined the infrared spectrum of the fully protiated mixture in a molar ratio of CER EOS/NS:CHOL:FA24:DPPC = 1:1:1:0.8. The scissoring vibrations are provided in Fig. 3F. This spectrum shows a central contour with a maximum at 1467 cm⁻¹ due to a hexagonal lateral packing. In addition, the two contours at 1463 cm⁻¹ and 1473 cm⁻¹ are also present. Obviously there is a coexistence of two phases: a fraction of lipids that adopts an orthorhombic packing, while another fraction assembles in a hexagonal packing.

3.2. Mixing of (perdeuterated) DPPC with SC lipids: interaction with lipids assembled in the SPP

The data are provided in the Supplement S2. Briefly, the CD₂ and CH₂ shifts indicate a mixing very similar to that presented for the lipids forming the LPP. When focusing on the scissoring vibrations at a high perdeuterated DPPC level a single peak at 1467 cm⁻¹ is observed demonstrating the nearly absence of skin lipid domains in an orthorhombic packing.

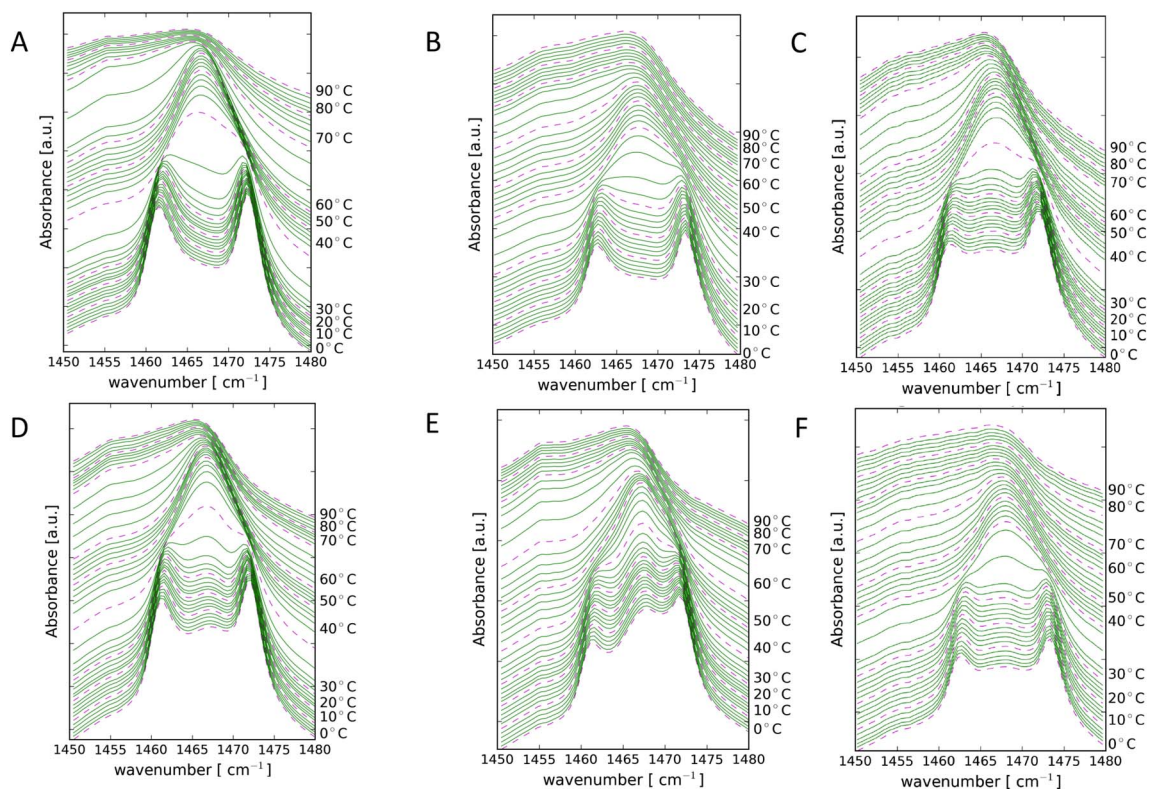


Fig. 3. Scissoring vibrations in the infrared spectra of CER EOS/NS:CHOL:FA24:DPPC mixtures with gradual increase in perdeuterated DPPC level. The spectra were measured between 0 and 90 °C. (A) CER EOS/NS:CHOL:FA24 = 1:1:1, (B) CER EOS/NS:CHOL:FA24:DPPC = 1:1:1:0.2, (C) CER EOS/NS:CHOL:FA24:DPPC = 1:1:1:0.6, (D) CER EOS/NS:CHOL:FA24:DPPC = 1:1:1:1 and (E) CER EOS/NS:CHOL:FA24:DPPC = 1:1:1:4 and (F) CER EOS/NS:CHOL:FA24:DPPC 1:1:1:0.8 (protiated). The dashed lines are scissoring vibrations after a rise in temperature of 10 °C.

3.3. Influence of DPPC on the long range ordering of the CER EOS/NS:CHOL:FA24 mixture

Besides the packing and ordering of the hydrocarbon chains, the long range ordering is also important. For this reason X-ray diffraction patterns were measured and the results are provided in Fig. 4. Already at a molar ratio of 1:1:1:0.2 phase separation occurred. The X-ray diffraction curve shows the 1st, 2nd, 3rd and 4th order diffraction peaks attributed to the LPP with a repeat distance of 12.5 nm, slightly longer compared to that of the 1:1:1:0 mixture being 12.3 nm. Two additional peaks indicate a second phase. Assuming that these are attributed to a lamellar phase, the repeat distance is around 6.05 nm. Furthermore, crystalline cholesterol is present indicated by two other reflections. At a ratio of 1:1:1:0.6 the repeat distance of the LPP is further increased to 12.7 nm. The 2nd order diffraction peak of the LPP is slightly asymmetric suggesting that another peak, most probably attributed to a DPPC-rich phase, is also present at approximately the same position. The reflections based on phase separated CHOL are reduced in intensity compared to that in the diffraction pattern of the 1:1:1:0.2 mixture. A further increase in DPPC content to an equimolar ratio increased the repeat distance of the LPP further to 12.9 nm. The 2nd order peak attributed to the LPP is very high in intensity compared to the 1st, 3rd and 4th order diffraction peak of this lamellar phase. This again suggests that another diffraction peak is present at the same position as that of the 2nd order peak of the LPP attributed to another phase. No phase separated CHOL could be detected. A further increase in the level of DPPC resulted in a disappearance of the reflections attributed to the LPP. The width of the diffraction peaks at half maximum is clearly increased demonstrating a less ordered long range ordering [23].

3.4. Influence of DPPC on the long range ordering of the CER NS:CHOL:FA24 mixture

The data are provided in the Supplement S2. Briefly, upon mixing with DPPC besides the SPP, a 2nd lamellar phase was formed. At very high DPPC levels the SPP disappeared.

3.5. Partitioning of DPPC into skin lipid mixtures prepared from CER EOS/NS:CHOL:FA24

As from the above results it is clear that DPPC and protiated SC lipids are partly participating in the same lattices, studies were performed in which the experimental set-up more closely resembles the topical application of a DPPC on the skin surface. In these studies a hydrated DPPC membrane and an hydrated equimolar CER EOS/NS:CHOL:FA24 SC lipid layer were sandwiched between two IR windows. This two-layer system was first equilibrated at 32 °C for 12 h keeping DPPC in a hexagonal packing. After equilibration the thermotropic response was measured between 0 and 90 °C. The CH₂ and CD₂ symmetric stretching frequencies are provided in Fig. 5A. The CD₂ symmetric stretching frequencies shift at around 35 °C from 2089 to 2093 cm⁻¹ indicating phase separated DPPC: perdeuterated DPPC is not partitioning into the skin lipid membrane. In the next study the equilibration temperature was shifted to 37 °C at which DPPC is in a liquid state (see Fig. 1) and the SC lipids are primarily in a hexagonal packing. The system was equilibrated for either 12 or 24 h. Again by monitoring the thermotropic response of the CH₂ and CD₂ stretching vibrations, mixing of DPPC with the SC lipids was examined. From Fig. 5B and C, it is obvious that equilibration at 37 °C results in a certain degree of mixing of DPPC with the SC lipids. After 12 h equilibration, there is a shift in the CD₂ symmetric stretching vibrations in the spectrum at around 35 °C from 2089 cm⁻¹ to 2092 cm⁻¹, but this shift

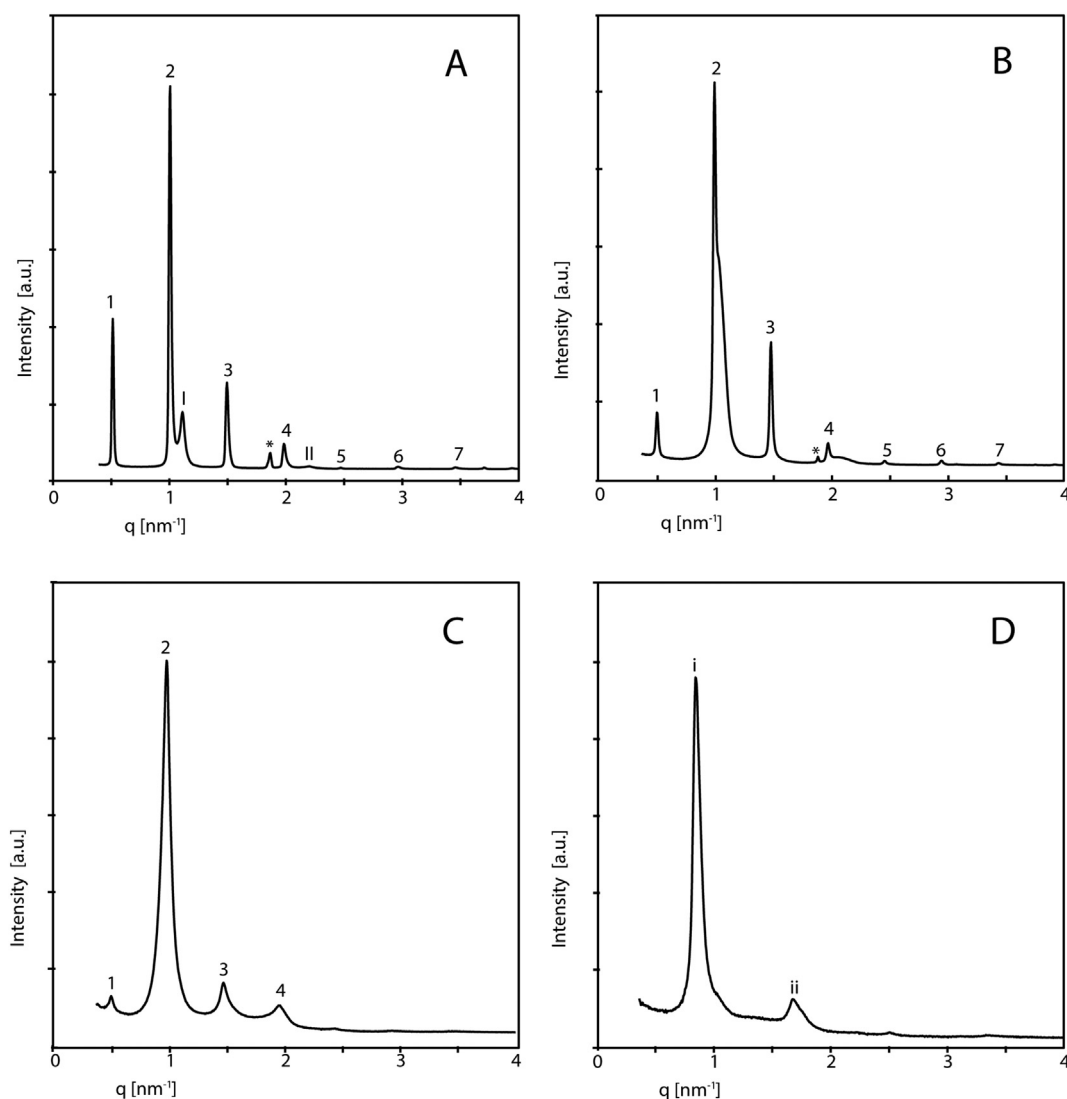


Fig. 4. The X-ray diffraction patterns of A) CER EOS/NS:CHOL:FA24:DPPC in a 1:1:1:0.2 M ratio, B) CER EOS/NS:CHOL:FA24:DPPC in a 1:1:1:0.6 M ratio, C) CER EOS/NS:CHOL:FA24:DPPC in a 1:1:1:1 M ratio and D) CER EOS/NS:CHOL:FA24:DPPC in a 1:1:1:4 M ratio. 1, 2, 3 and 4 denotes the four diffraction peaks attributed to the LPP. I and i refer to another phase, most probably a DPPC rich phase. The additional peak close to the 3rd order of the LPP in panel A is attributed to an unknown phase.

extends over a very wide temperature interval and at the temperature region at which the hexagonal-liquid phase transition of the SC lipids occurs (around 60–70 °C), again a stronger shift in the CD_2 frequency occurs. This demonstrates that a fraction of the DPPC is mixing with the SC lipids. Extending the equilibration period to 24 h (at 37 °C) and subsequently measuring the thermotropic response, the CD_2 stretching frequencies show that the DPPC phase transition occurs in the same region at which the hexagonal-liquid phase transition of the protiated lipids occurred. As between the equilibrium temperatures of 32 °C and 37 °C, two phase changes occur 1) DPPC is in a hexagonal phase at 32 °C and in a liquid phase at 37 °C, and 2) the SC lipids transform from an orthorhombic to a hexagonal lateral packing. As it is known that the DPPC:CHOL mixture forms a liquid-ordered phase, DPPC:CHOL in a 2:1 M ratio was equilibrated with the SC lipids at 32 °C for 24 h [24]. Again, the FTIR spectra were monitored between 0 and 90 °C. The CH_2 and CD_2 thermotropic responses are provided in Fig. 5D. No shift in the CD_2 stretching vibrations similar to that in a DPPC:CHOL spectrum (not shown, but a steady increase in CD_2 stretching frequencies between 20 and 80 °C having a value of 2093 cm^{-1} at 60 °C), instead the CD_2 shift occurred in the same temperature region as the CH_2 shift of the SC lipids.

4. Discussion

As there is almost no information describing the molecular interactions of specific phospholipids with SC lipids, while phospholipids (particularly lecithin) are frequently used in topical formulations, it was decided to study the interaction between pure DPPC and synthetic well-defined SC lipid mixtures. DPPC was selected as this is a frequently used phospholipid, it has excellent physico-chemical properties to study the interactions with SC lipids and perdeuterated DPPC is commercial available. In the present studies we used two simple SC lipid mixtures: i) CER EOS/NS:CHOL:FA24 with a CER composition of 40% CER EOS and 60% CER NS. This composition forms only the LPP and ii) CER NS:CHOL:FA24 forming only the SPP. We chose for these compositions as this allowed us to study the interaction of DPPC with each of the lamellar phases separately. When reducing the level of CER EOS to around 10–15%, a similar level of all acyl-CERs as present in SC, the two lamellar phases coexist in the lipid mixture, in which each of the lamellar phases is very similar to those in the present study (see Supplement S4). Until now self-assembling of SC lipids into only the LPP was reported with multi-component mixtures [25–27]. However, in the present study for the first time we show that the LPP can be formed with only a 4 component system in the absence of other lamellar

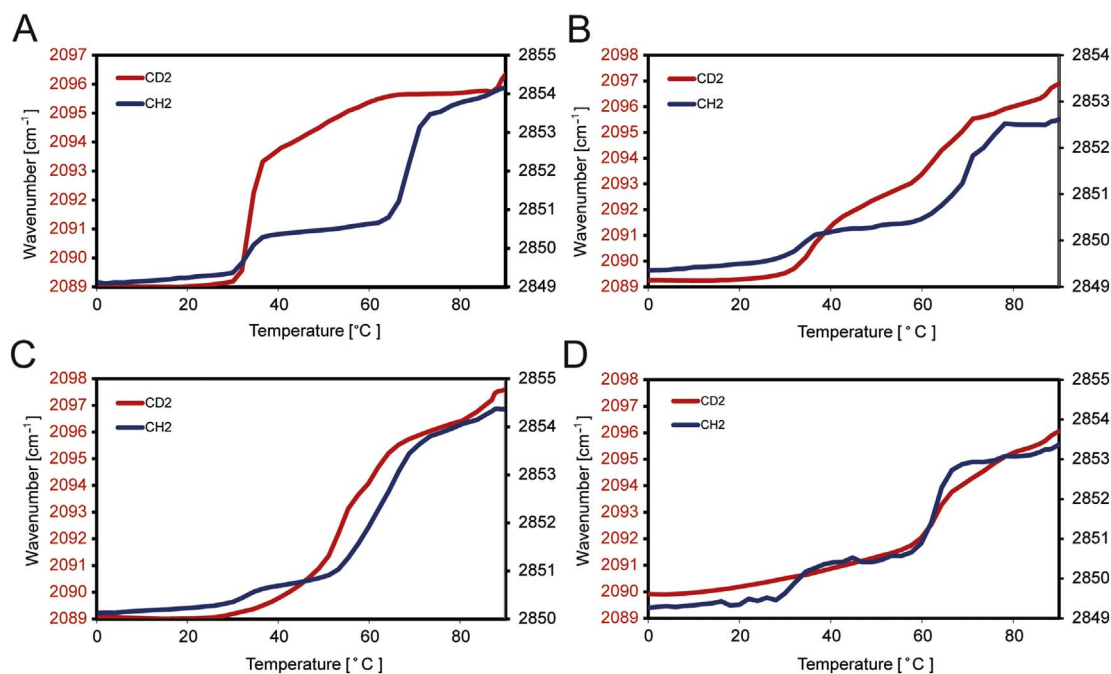


Fig. 5. CH₂ and CD₂ symmetric stretching vibrations after equilibration of perdeuterated DPPC on a skin lipid membrane at A) 32 °C for 12 h, B) 37 °C for 12 h, C) 37 °C for 24 h. D) CH₂ and CD₂ symmetric stretching vibrations after equilibration of a mixture of DPPC:CHOL at the skin lipid membrane at 32 °C for 24 h.

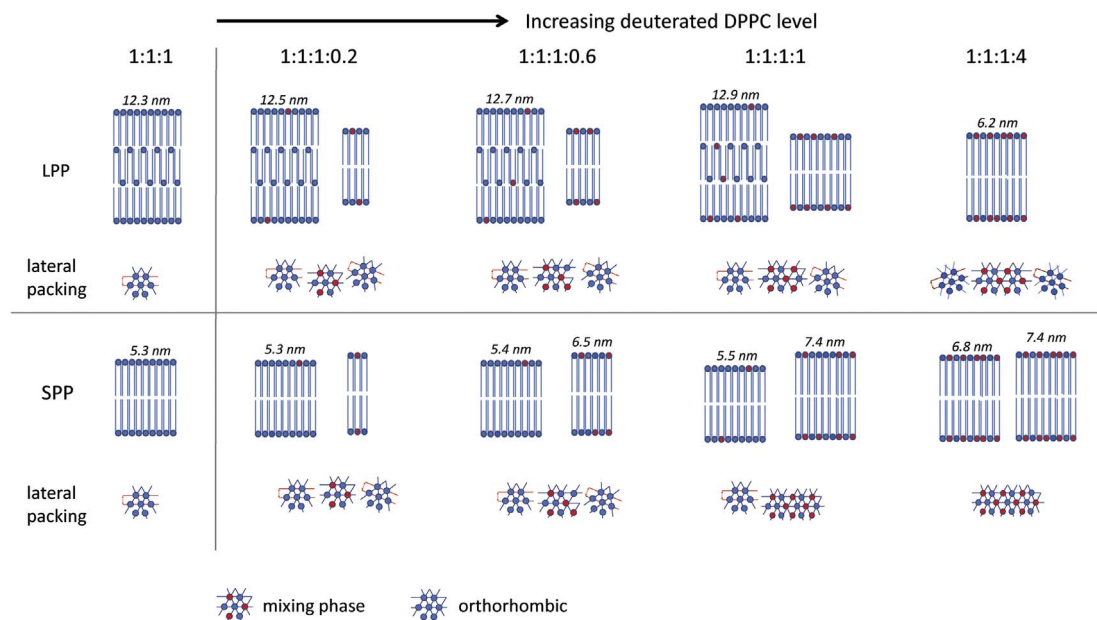


Fig. 6. A model of the induced changes in phase behaviour when increasing the DPPC level in lipids forming initially the long periodicity phase (LPP) or the short periodicity phase (SPP). The ratios provided are the ratios between CER (EOS/NS or NS): CHOL:FA24:DPPC. The red head-groups indicate perdeuterated DPPC. The blue head-groups refer to the SC lipids.

phases. The repeat distance as well as the intensity distribution of the diffraction peaks are very similar to that reported for the complex system consisting of 5 CER subclasses and a broad distribution of fatty acid chain lengths [12] suggesting that not only the repeat distance, but also the electron density distribution in the repeating unit is very similar in the simple and complex systems. In a previous study using a similar composition this was not observed [27]. This may be due to either the presence of cholesterol sulfate, or a different equilibration procedure. The former is highly unlikely: a low level of cholesterol sulfate comparable to that in healthy skin does not affect the lamellar phases [28]. The effect of DPPC on the lipid phase behaviour and a comparison with penetration enhancers is discussed below. To facilitate the discussions a schematic view of the observed phase behaviour with

increasing amount of DPPC in the skin lipid mixtures is provided in Fig. 6.

4.1. Mixtures prepared with (perdeuterated) DPPC and SC lipids

There are a number of publications reporting the phase behaviour of DPPC:CER:CHOL mixtures and sphingomyelin:CER:CHOL mixtures. Concerning the latter the focus is often the competition between CHOL and CER, both being hydrophobic components with small head groups that are able to interact with the amide group of sphingomyelin forming a network of hydrogen bondings. These studies are of interest as these interactions play a role in the formation of rafts in cell-membrane systems. An excellent review describing these mixtures has been

published recently [29]. In DPPC and CER mixtures favourable interactions have been reported between the two lipid classes at low CER levels [30]. Interactions of saturated levels of CER and CHOL in POPC (1-palmitol-2-oleylphosphatidylcholine) bilayers were also examined [31] and it was reported that the solubility of CHOL in the DOPC bilayer reduced when increasing the CER level demonstrating a strong interaction between the hydrophobic CER and the hydrophilic phospholipid [31]. Important to mention is that in these studies the CER molecular architecture was slightly different from those in the present studies: shorter CER chain lengths and when brain CER were used, a fraction of the chains are unsaturated.

4.1.1. Absence of pure DPPC domains

In the present studies when DPPC was mixed with SC lipids prior to self-assembling of the lipid mixtures on a support, DPPC interacted with SC lipids and even at very high DPPC level, no phase separated pure DPPC was detected with FTIR. This was observed for mixtures prepared with either CER EOS/NS:CHOL:FA24 or CER NS:CHOL:FA24. This high miscibility may be enhanced by the strong interactions reported between DPPC and CER as mentioned above [29–31]. That no pure DPPC domains are present can be inferred from the CH₂ and CD₂ stretching vibrations: no shift in the CD₂ stretching vibrations was shown in the spectra at a temperature of around 36 °C, the order-disorder transition temperature of pure hydrated DPPC. Instead, a concerted transition from hexagonal to liquid-phase occurred for the protiated SC lipids and the perdeuterated DPPC at elevated temperatures. This demonstrates that the SC lipids dictate the DPPC transition from hexagonal to liquid phase even at very high levels of DPPC. Another interesting feature is the sensitivity of the CH₂ symmetric stretching vibrations for the perdeuterated DPPC mixtures: the presence of perdeuterated DPPC results in general in an increase in the CH₂ stretching vibration compared to the control. This may at least partly be caused by only the presence of perdeuterated chains of DPPC affecting the CH₂ vibrations as described previously using isotopic dilution experiments [32]. In addition DPPC itself due to its bulky head group and short chain length may increase the disordering of the protiated hydrocarbon chains.

The X-ray diffraction results demonstrate that DPPC and SC lipids assemble into at least two phases. One phase is either the SPP or the LPP (exception is the 1:1:1.4 M ratio) The additional phase is most likely a DPPC-rich phase, in which also ceramides, fatty acids and cholesterol may participate as no phase separated domains of DPPC could be identified.

4.1.2. Mixing properties of DPPC and SC lipids

Focusing on the CH₂ scissoring vibrations, the results demonstrate that DPPC and SC lipids participate in the same lattices. This was shown for the CER EOS/NS:CHOL:FA24 as well as the CER NS:CHOL:FA24 mixtures. This conclusion is based on the formation of a central contour in the CH₂ scissoring frequency region of the spectra and the absence of the shift at around 36 °C in the thermotropic responses of the CD₂ stretching frequencies. As this central peak was also present in the fully protiated sample, DPPC mixes with SC lipids thereby forcing a fraction of the SC lipids to adopt a hexagonal packing. Besides the LPP or SPP, the additional long range ordered phase was already present in the 1:1:1:0.2 composition of both the CER EOS/NS:CHOL:FA24:DPPC and CER NS:CHOL:FA24:DPPC mixtures, while no clear hexagonal packing was observed at these low DPPC levels. Therefore, the additional long range ordering phase cannot directly be related to the hexagonal packing. However, at higher DPPC levels most of the lipids adopting the hexagonal packing are expected to be in the DPPC-rich phase.

Whether a fraction of DPPC forms together with the SC lipids a dense orthorhombic packing cannot be concluded from the scissoring frequencies. However, when focusing on the lipid mixture forming an LPP, a gradual increase in the repeat distance was observed when increasing the level of DPPC. Furthermore, only a clear scissoring band at 1467 cm⁻¹ was detected in the scissoring frequency spectrum at a

DPPC level higher than 1:1:1:0.6. These observations strongly suggest that DPPC is at least partly incorporated in the unit cell of the LPP. Participation of DPPC in the LPP is quite remarkable: the size of the DPPC head group is very bulky compared to the CER head group and in hydrated state DPPC attracts around 22 water molecules [33], while a ceramide molecule attracts only 1 or 2 water molecules [34,35]. Furthermore the chain length of DPPC is only 16 carbon atoms, while the length of the fatty acid and acyl chain of CER NS is 24 carbon atoms. The incorporation of the DPPC may be enhanced by the presence of the linoleate moiety of CER EOS, as this unsaturated acyl chain is located close to the inner head group regions in the unit cell of this phase and the strong interaction between CERs and DPPC [26,31]. There was only a very small gradual increase in repeat distance of the SPP when increasing the DPPC level in the CER NS:CHOL:FFA mixture. In addition no central CH₂ scissoring peak at 1467 cm⁻¹ is formed at DPPC levels below 1:1:1:0.6, while both the SPP and the orthorhombic packing disappear at the CER NS:CHOL:FFA:DPPC ratio of 1:1:1:4. This may indicate that the orthorhombic lateral packing is related to the SPP and that the level of DPPC participating in the SPP is very limited. In mixtures with high level of DMPC and low level of phytosphingosine-based CERs, changes in repeat distances were reported [36]. However, these were very different compositions.

In the present study a limited number of CER subclasses with only a 30 or 24 carbon atom in the acyl chain only a single FA with a chain length of 24 carbon atoms have been used. However, when using 5 CER subclasses and 7 fatty acids differing in chain length between C16 and C26, the lipids assemble in very similar lamellar phases with repeat distances of 5.3 and 12.3 nm [12,37]. Even when comparing the phase behaviour between the simple synthetic mixtures and isolated CERs mixed with CHOL and FFAs, a similar phase behaviour was observed. In these mixtures a wide chain length distribution of the CERs is encountered [38]. A wider chain length distribution is expected to facilitate the mixing between DPPC and the SC lipid mixtures.

4.1.3. Comparison of DPPC with penetration enhancers and moisturisers

When comparing the interactions between DPPC and SC lipids with those observed between penetration enhancers or moisturisers and SC lipids, differences are detected. Penetration enhancers that are effective in enhancing the transport of molecules across the SC, such as oleic acid, oleyl-azone and dodecyl-azone frequently show phase separation, in which enhancer-rich liquid domains are present in crystalline phases [39–42]. These enhancers have either a short chain length or are unsaturated. These chain characteristics plays a role in this phase behaviour. In contrast as an example a lipophilic moisturiser iso-stearylisostearate increases the lattice density by mixing with the SC lipids and thereby enhancing an orthorhombic packing and reducing the permeability of water [43]. The small hydrophilic head group along with the increased chain length may be responsible for creating the dense structure. The interactions of the penetration enhancers and moisturiser are different from those between DPPC and SC lipids. The strong interaction between the head groups of DPPC CERs may facilitate the mixing between the lipids. However, the DPPC head group architecture, especially its size [33], may play a role in enhancing the formation of the hexagonal phase induced by DPPC.

4.2. Topical application of DPPC

The mixing of DPPC and SC lipids, although of interest to study, does not mimic the situation when applying a topical formulation onto the skin, as in the latter partitioning into the SC lipid matrix is required prior to mixing. For this reason it was decided to perform studies in which hydrated DPPC was placed directly on top of the model SC lipids. Only when DPPC partitions into the skin lipid matrix, or the SC lipids partition into the DPPC layer interactions between DPPC and SC lipids will occur. As in these studies pure DPPC was used, in our settings at the

start of the studies, the DPPC has the maximum driving force to partition into the SC lipid matrix.

When applying DPPC on top of a SC lipid membrane, our studies show that DPPC in a liquid crystalline state partitions into the SC lipid membrane and subsequently interacts with the SC lipids. Simultaneously, most probably, CHOL, FA24 and CERs partition into the DPPC layer as well. The partitioning is quite fast as after 24 h no phase separated DPPC remained. In contrast to DPPC in a liquid phase, when DPPC was in a rippled-gel phase, almost no partitioning and mixing occurred within a period of 24 h. In a previous study mixing between two populations of vesicles prepared from either DPPC/CHOL and skin lipids was examined and it was shown that mixing between DPPC and skin lipid vesicles also occurred within 24 h [44]. This is very similar to our results. However, in our studies there was a direct contact between DPPC and the SC lipids and the composition of the SC lipids was very different. As SC lipids undergo a transition from orthorhombic to hexagonal packing between 32 °C and 37 °C [45,46], the difference in interaction between SC lipids and DPPC at these temperatures may also be attributed to the SC lipid orthorhombic-hexagonal phase change. However, when applying DPPC:CHOL in a liquid ordered (L_o) phase at 32 °C on top of the SC lipids partitioning of DPPC occurred indicating the ability to partition into the SC lipid matrix is mainly due to the change in DPPC phase.

4.2.1. Consequences for the phospholipid containing topical formulations

When extrapolating our results to topical formulations, there are two important issues, namely I) when phospholipids are applied in liquid (L_α or L_o) state onto the skin surface, partitioning of the phospholipids into the SC lipid matrix can be expected thereby inducing a hexagonal lateral packing. Increasing the fraction of lipids forming a hexagonal packing in the SC will reduce the skin barrier as observed for water, benzoic acid and hydrocortisone [18,47]. Whether indeed the applied phospholipids will reduce the skin barrier depends on the amount of phospholipids that will partition into the SC lipid matrix and the subsequent penetration into the deeper layers of the SC establishing a concentration gradient. Based on the expected higher abundance of phospholipids in the superficial layers in the SC, it is likely that in this layer a hexagonal packing will be more abundantly present than in the deeper SC layers. When applying phospholipids in a gel phase in the formulation, it is not expected to partition into the SC lipid matrix and II) it has been reported and reviewed that differences in skin permeation and skin lipid interactions occur between gel-state and liquid-state liposomes topically applied onto skin [48,49]. The present study shows that this may not only be due to a difference in fusion process of the liposomes on the skin surface, but may also be caused by a difference in the ability of single phospholipid species to partition into the ordered SC lipid matrix. Although the work to date has focused on simplified single component phospholipid systems it is certain that phospholipid chain length and head group architecture also play a role in determining the extent of interaction between topical phospholipids and skin barrier lipids. Clearly further studies are necessary to improve our understanding of the interaction between topically applied phospholipids and SC lipids.

Authors' contributions

G.S. Gooris: Designed research, performed research, analysed data.
 M. Kamran: Designed research, performed research, analysed data.
 A. Kros: Designed research, contributed analysing data.
 D.J. Moore: Designed research, Contributed analysing data, wrote paper.
 J.A. Bouwstra: Designed research, contributed analysing data, wrote paper.

Transparency document

The <http://dx.doi.org/10.1016/j.bbamem.2018.02.024> associated with this article can be found, in the online version.

Acknowledgements

We like to thank GSK for financing the research described in this paper. We like to thank the company Evonik (Essen, Germany) for their generous provision of CERs. We also like to thank the personnel at the Dutch Belgium beam Line at the ESRF in Grenoble, France for their assistance and allocation of beam time for X-ray diffraction measurements.

Appendix A. Supplementary data

Supplementary data to this article can be found online at <https://doi.org/10.1016/j.bbamem.2018.02.024>.

References

- [1] D.J. McClements, C.E. Gumus, Natural emulsifiers - biosurfactants, phospholipids, biopolymers, and colloidal particles: molecular and physicochemical basis of functional performance, *Adv. Colloid Interf. Sci.* 234 (2016) 3–26.
- [2] C.R. Harding, A. Watkinson, A.V. Rawlings, I.R. Scott, Dry skin, moisturization and corneodesmolysis, *Int. J. Cosmet. Sci.* 22 (2000) 21–52.
- [3] J. van Smeden, M. Janssens, G.S. Gooris, J.A. Bouwstra, The important role of stratum corneum lipids for the cutaneous barrier function, *Biochim. Biophys. Acta* 1841 (2014) 295–313.
- [4] J.A. Bouwstra, G.S. Gooris, J.A. van der Spek, W. Bras, Structural investigations of human stratum corneum by small-angle X-ray scattering, *J. Invest. Dermatol.* 97 (1991) 1005–1012.
- [5] R.O. Potts, V.H. Mak, R.H. Guy, M.L. Francoeur, Strategies to enhance permeability via stratum corneum lipid pathways, *Adv. Lipid Res.* 24 (1991) 173–210.
- [6] T.M. Suhonen, J.A. Bouwstra, A. Urtti, Chemical enhancement of percutaneous absorption in relation to stratum corneum structural alterations, *J. Control. Release* 59 (1999) 149–161.
- [7] P.A. Cornwell, B.W. Barry, C.P. Stoddart, J.A. Bouwstra, Wide angle X-ray diffraction of human stratum corneum: effect of hydration and terpene enhancer treatment, *J. Pharm. Pharmacol.* 46 (12) (1994) 938–950.
- [8] Y. Masukawa, H. Narita, E. Shimizu, N. Kondo, Y. Sugai, T. Oba, R. Homma, J. Ishikawa, Y. Takagi, T. Kitahara, Y. Takema, K. Kita, Characterization of overall ceramide species in human stratum corneum, *J. Lipid Res.* 49 (2008) 1466–1476.
- [9] R. t'Kindt, L. Jorge, E. Dumont, P. Couturon, F. David, P. Sandra, K. Sandra, Profiling and characterizing skin ceramides using reversed-phase liquid chromatography-quadrupole time-of-flight mass spectrometry, *Anal. Chem.* 84 (2012) 403–411.
- [10] J. van Smeden, L. Hoppel, R. van der Heijden, T. Hankemeier, R.J. Vreeken, J.A. Bouwstra, LC/MS analysis of stratum corneum lipids: ceramide profiling and discovery, *J. Lipid Res.* 52 (2011) 1211–1221.
- [11] M. Rabionet, A. Bayerle, C. Marsching, R. Jennemann, H.J. Grone, Y. Yildiz, D. Wachten, W. Shaw, J.A. Shayman, R. Sandhoff, 1-O-acylceramides are natural components of human and mouse epidermis, *J. Lipid Res.* 54 (2013) 3312–3321.
- [12] E.H. Mojumdar, G.S. Gooris, J.A. Bouwstra, Phase behavior of skin lipid mixtures: the effect of cholesterol on lipid organization, *Soft Matter* 11 (2015) 4326–4336.
- [13] M. Uchiyama, M. Oguri, E.H. Mojumdar, G.S. Gooris, J.A. Bouwstra, Free fatty acids chain length distribution affects the permeability of skin lipid model membranes, *Biochim. Biophys. Acta* 1858 (2016) 2050–2059.
- [14] N. Kitson, J. Thewalt, M. Lafleur, M. Bloom, A model membrane approach to the epidermal permeability barrier, *Biochemistry* 33 (1994) 6707–6715.
- [15] X. Chen, S. Kwak, M. Lafleur, M. Bloom, N. Kitson, J. Thewalt, Fatty acids influence “solid” phase formation in models of stratum corneum intercellular membranes, *Langmuir* 23 (2007) 5548–5556.
- [16] D.J. Moore, R.G. Snyder, M.E. Rerek, R. Mendelsohn, Kinetics of membrane raft formation: fatty acid domains in stratum corneum lipid models, *J. Phys. Chem. B* 110 (2006) 2378–2386.
- [17] M.R. Vist, J.H. Davis, Phase equilibria of cholesterol/dipalmitoylphosphatidylcholine mixtures: 2H nuclear magnetic resonance and differential scanning calorimetry, *Biochemistry* 29 (1990) 451–464.
- [18] E.H. Mojumdar, R.W. Helder, G.S. Gooris, J.A. Bouwstra, Monounsaturated fatty acids reduce the barrier of stratum corneum lipid membranes by enhancing the formation of a hexagonal lateral packing, *Langmuir* 30 (2014) 6534–6543.
- [19] W. Bras, I.P. Dolbnya, D. Detollenaere, R. van Tol, M. Malfois, G.N. Greaves, A.J. Ryan, E. Heeley, Recent experiments on a combined small-angle/wide-angle X-ray scattering beam line at the ESRF, *J. Appl. Crystallogr.* 36 (2003) 791–794.
- [20] D.J. Moore, M.E. Rerek, R. Mendelsohn, Lipid domains and orthorhombic phases in model stratum corneum: evidence from Fourier transform infrared spectroscopy studies, *Biochem. Biophys. Res. Commun.* 231 (1997) 797–801.
- [21] D.J. Moore, R.H. Sills, R. Mendelsohn, Conformational order of specific

- phospholipids in human erythrocytes: correlations with changes in cell shape, *Biochemistry* 36 (1997) 660–664.
- [22] R.G. Snyder, G.L. Liang, H.L. Strauss, R. Mendelsohn, IR spectroscopic study of the structure and phase behavior of long-chain diacylphosphatidylcholines in the gel state, *Biophys. J.* 71 (1996) 3186–3198.
- [23] A.E. Blaurock, J.C. Nelander, Disorder in nerve myelin: analysis of the diffuse x-ray scattering, *J. Mol. Biol.* 103 (1976) 421–431.
- [24] D. Marsh, Liquid-ordered phases induced by cholesterol: a compendium of binary phase diagrams, *Biochim. Biophys. Acta* 1798 (2010) 688–699.
- [25] A. Eichner, S. Sonnenberger, B. Dobner, T. Hauss, A. Schroeter, R.H. Neubert, Localization of methyl-branched ceramide [EOS] species within the long-periodicity phase in stratum corneum lipid model membranes: a neutron diffraction study, *Biochim. Biophys. Acta* 1858 (2016) 2911–2922.
- [26] E.H. Mojumdar, G.S. Gooris, D. Groen, D.J. Barlow, M.J. Lawrence, B. Deme, J.A. Bouwstra, Stratum corneum lipid matrix: location of acyl ceramide and cholesterol in the unit cell of the long periodicity phase, *Biochim. Biophys. Acta* 1858 (2016) 1926–1934.
- [27] L. Opalka, A. Kovacic, J. Maixner, K. Vavrova, Omega-O-acylceramides in skin lipid membranes: effects of concentration, sphingoid base, and model complexity on microstructure and permeability, *Langmuir* 32 (2016) 12894–12904.
- [28] A. Weerheim, M. Ponec, Determination of stratum corneum lipid profile by tape stripping in combination with high-performance thin-layer chromatography, *Arch. Dermatol. Res.* 293 (2001) 191–199.
- [29] A.B. Garcia-Arribas, A. Alonso, F.M. Goni, Cholesterol interactions with ceramide and sphingomyelin, *Chem. Phys. Lipids* 199 (2016) 26–34.
- [30] D.C. Carrer, B. Maggio, Phase behavior and molecular interactions in mixtures of ceramide with dipalmitoylphosphatidylcholine, *J. Lipid Res.* 40 (1999) 1978–1989.
- [31] M.R. Ali, K.H. Cheng, J. Huang, Ceramide drives cholesterol out of the ordered lipid bilayer phase into the crystal phase in 1-palmitoyl-2-oleoyl-sn-glycero-3-phosphocholine/cholesterol/ceramide ternary mixtures, *Biochemistry* 45 (2006) 12629–12638.
- [32] V.R. Kodati, R. Eljastimi, M. Lafleur, Contribution of the intermolecular coupling and librational mobility in the methylene stretching modes in the infrared-spectra of acyl chains, *J. Phys. Chem.* 98 (1994) 12191–12197.
- [33] M. Pasenkiewicz-Gierula, Y. Takaoka, H. Miyagawa, K. Kitamura, A. Kusumi, Hydrogen bonding of water to phosphatidylcholine in the membrane as studied by a molecular dynamics simulation: location, geometry, and lipid–lipid bridging via hydrogen-bonded water, *J. Phys. Chem. A* 101 (1997) 3677–3691.
- [34] A. Schroter, D. Kessner, M.A. Kiselev, T. Hauss, S. Dante, R.H. Neubert, Basic nanostructure of stratum corneum lipid matrices based on ceramides [EOS] and [AP]: a neutron diffraction study, *Biophys. J.* 97 (2009) 1104–1114.
- [35] D. Groen, G.S. Gooris, D.J. Barlow, M.J. Lawrence, J.B. van Mechelen, B. Deme, J.A. Bouwstra, Disposition of ceramide in model lipid membranes determined by neutron diffraction, *Biophys. J.* 100 (2011) 1481–1489.
- [36] J. Zbytovska, M.A. Kiselev, S.S. Funari, V.M. Garamus, S. Wartewig, R. Neubert, Influence of phytosphingosine-type ceramides on the structure of DMPC membrane, *Chem. Phys. Lipids* 138 (2005) 69–80.
- [37] M. de Jager, G. Gooris, M. Ponec, J. Bouwstra, Acylceramide head group architecture affects lipid organization in synthetic ceramide mixtures, *J. Investig. Dermatol.* 123 (2004) 911–916.
- [38] J.A. Bouwstra, G.S. Gooris, F.E. Dubbelaar, M. Ponec, Phase behavior of lipid mixtures based on human ceramides: coexistence of crystalline and liquid phases, *J. Lipid Res.* 42 (2001) 1759–1770.
- [39] G.S. Pilgram, A.M. Engelsma-van Pelt, H.K. Koerten, J.A. Bouwstra, The effect of two azones on the lateral lipid organization of human stratum corneum and its permeability, *Pharm. Res.* 17 (2000) 796–802.
- [40] J.A. Bouwstra, B.A. van den Bergh, M. Suhonen, Topical application of drugs: mechanisms involved in chemical enhancement, *J. Recept. Signal Transduct. Res.* 21 (2001) 259–286.
- [41] A.C. Williams, B.W. Barry, Penetration enhancers, *Adv. Drug Deliv. Rev.* 56 (2004) 603–618.
- [42] B. Ongpipattanakul, R.R. Burnette, R.O. Potts, M.L. Francoeur, Evidence that oleic acid exists in a separate phase within stratum corneum lipids, *Pharm. Res.* 8 (1991) 350–354.
- [43] J. Caussin, G.S. Gooris, J.A. Bouwstra, FTIR studies show lipophilic moisturizers to interact with stratum corneum lipids, rendering the more densely packed, *Biochim. Biophys. Acta* 1778 (2008) 1517–1524.
- [44] A. Blume, M. Jansen, M. Ghyczy, J. Gareiss, Interaction of phospholipid liposomes with lipid model mixtures for stratum-corneum lipids, *Int. J. Pharm.* 99 (1993) 219–228.
- [45] S.H. White, D. Mirejovsky, G.I. King, Structure of lamellar lipid domains and corneocyte envelopes of murine stratum corneum. An X-ray diffraction study, *Biochemistry* 27 (1988) 3725–3732.
- [46] J.A. Bouwstra, M. Ponec, The skin barrier in healthy and diseased state, *Biochim. Biophys. Acta* 1758 (2006) 2080–2095.
- [47] F. Damien, M. Boncheva, The extent of orthorhombic lipid phases in the stratum corneum determines the barrier efficiency of human skin in vivo, *J. Invest. Dermatol.* 130 (2010) 611–614.
- [48] N.O. Knudsen, L. Jorgensen, J. Hansen, C. Vermehren, S. Frokjaer, C. Foged, Targeting of liposome-associated calcipotriol to the skin: effect of liposomal membrane fluidity and skin barrier integrity, *Int. J. Pharm.* 416 (2011) 478–485.
- [49] C. Xiao, D.J. Moore, M.E. Rerek, C.R. Flach, R. Mendelsohn, Feasibility of tracking phospholipid permeation into skin using infrared and Raman microscopic imaging, *J. Investig. Dermatol.* 124 (2005) 622–632.